

Supporting Information

to

Protein docking using an ensemble of spin labels optimized by intra-molecular paramagnetic relaxation enhancement.

Jesika Schilder,¹ Wei-Min Liu,¹ Pravin Kumar,² Mark Overhand,¹ Martina Huber² and Marcellus Ubbink.¹

¹Leiden Institute of Chemistry, Leiden University, Gorlaeus Laboratories, Einsteinweg 55, 2333 CC Leiden, The Netherlands

²Department of Physics, Huygens-Kamerlingh Onnes Laboratory, Leiden University, Niels Bohrweg 2, 2333 CA Leiden, The Netherlands

Table S1: Intramolecular PRE ($R_{2,\text{para}}$) values for CcP C128A amide protons within 23 Å of the paramagnetic centre in MTSL or pyMTSL attached at positions 38, 200 or 288 on CcP. The PRE were measured while CcP was in a 1:1 complex with Cc.

Residue	<u>38C</u>		<u>200C</u>			<u>288C</u>		
	MTSL $R_{2,\text{para}}$ (s^{-1})	pyMTSL $R_{2,\text{para}}$ (s^{-1})	Residue	MTSL $R_{2,\text{para}}$ (s^{-1})	pyMTSL $R_{2,\text{para}}$ (s^{-1})	Residue	MTSL $R_{2,\text{para}}$ (s^{-1})	pyMTSL $R_{2,\text{para}}$ (s^{-1})
33	15.6	13.1	30	4.5	-	16	12.5	7.4
34	45.9	39.8	31	2.9	-	17	12.3	11.4
37	137.1	185.8	34	10.1	-	19	4.8	15.2
38	231.4	266.1	39	0.0	0.0	20	37.1	19.6
41	94.6	80.7	40	6.6	7.1	21	20.6	29.3
42	45.2	38.3	41	11.4	10.3	25	0.0	0.0
43	38.8	26.0	42	9.3	-	33	3.1	2.9
84	34.3	26.4	43	12.1	11.0	34	22.1	19.6
86	18.0	-	112	4.7	1.3	41	21.9	14.9
87	37.6	40.2	115	82.1	66.6	42	40.4	28.1
88	28.7	19.5	117	26.0	24.4	43	58.0	40.4
90	8.2	-	118	27.1	44.2	91	0.0	0.0
91	16.5	12.1	119	17.9	9.3	92	13.4	-
180	4.7	4.1	120	71.8	68.0	95	0.0	0.0
181	5.0	0.3	121	104.2	70.0	110	0.0	0.0
182	106.8	100.3	123	26.3	23.2	120	113.5	88.1
183	80.3	89.4	124	0.0	-	123	181.3	150.6
184	10.3	11.2	126	2.3	-	124	69.7	44.8
186	51.6	42.6	165	29.1	23.1	128	2.9	-
188	4.7	8.4	166	14.4	6.3	170	19.4	15
194	6.5	0.9	167	13.3	5.2	194	0.0	3.0
205	12.2	0.0	168	7.7	8.4	197	0.0	0.0
216	20.8	15.8	169	24.8	8.8	198	39.6	41.6
217	12.8	10.4	170	28.1	30.3	199	129.9	87.7
218	24.3	11.8	173	245.5	18.8	200	144.8	36.5
223	20.1	24.4	189	16.5	-	201	102.3	82.6
224	8.3	8.6	196	197.6	139.6	202	22.6	14.3
225	39.6	28.2	198	66.8	55.2	205	11.2	-
226	18.5	17.9	199	246.3	185.8	250	3.5	8.9
227	32.3	26.9	202	242.3	182.0	251	12.3	0.0
228	66.7	53.7	204	174.1	117.6	252	11.8	22.4
230	9.1	0.0	206	166.7	127.0	253	19.6	24.6
			207	108.5	111.2	255	104.3	84.1
			208	19.3	14.4	256	108.1	123.7
			209	110.4	92.7	257	77.3	94.5
			210	32.6	31.8	259	87.1	87.9
			211	0.0	0.0	260	52.1	36.6
			225	24.0	24.8	262	141.8	68.3
			226	53.0	22.6	263	133.7	55.1
			227	49.0	41.0	264	83.7	89.2
			228	38.8	36.1	284	41.0	24.7
			230	16.1	61.1	285	120.2	98.2
			231	14.7	11.9	287	269.5	270.5
			235	9.3	3.7			
			236	7.2	0.0			

238	-	9.1
239	-	9.6
244	8.7	11.0
245	11.1	14.0
246	18.1	18.8
247	27.1	23.1
248	103.4	52.1
250	85.1	79.2
251	375.7	309.5
253	212.6	153.8
254	179.3	155.0
256	191.0	124.3
257	349.6	285.2
258	313.5	250.2
259	131.9	152.4
260	95.1	84.8
261	65.1	70.6
262	54.9	49.5
263	33.9	40.5
264	22.8	22.0
265	23.2	0.0
266	12.9	13.7
267	9.7	14.9
285	38.6	15.3
286	7.0	4.5
287	4.2	16.3
288	10.0	7.2
289	6.5	2.8
290	10.8	8.3
291	21.4	25.6
292	10.0	12.8
293	5.3	6.4
294	6.3	-

Table S2: Intermolecular PRE ($R_{2,\text{para}}$) values for Cc amide protons generated by the paramagnetic centre in MTSL or pyMTSL attached at positions 38, 200 or 288 on CcP. The PRE were measured while CcP was in a 1:1 complex with Cc.

Residue	<u>38C</u>		<u>200C</u>		<u>288C</u>	
	MTSL $R_{2,\text{para}}$ (s^{-1})	pyMTSL $R_{2,\text{para}}$ (s^{-1})	MTSL $R_{2,\text{para}}$ (s^{-1})	pyMTSL $R_{2,\text{para}}$ (s^{-1})	MTSL $R_{2,\text{para}}$ (s^{-1})	pyMTSL $R_{2,\text{para}}$ (s^{-1})
1	2.6	1.4	0.0	0.0	0.9	0.6
2	22.7	18.4	0.0	0.0	1.4	12.2
4	22.5	20.5	8.4	6.0	3.3	3.8
5	327.0	375.5	15.7	6.3	3.7	1.5
6	85.1	61.2	11.1	4.5	3.6	3.2
7	333.9	381.4	26.9	11.2	5.7	4.6
8	330.3	377.9	144.0	48.9	6.0	5.4
9	292.8	339.6	81.0	34.9	12.8	7.8
10	352.5	400.5	68.3	35.3	8.6	5.7
11	344.3	392.3	407.1	356.9	13.7	6.8
12	264.8	311.2	327.7	279.6	28.9	22.9
13	312.4	359.8	114.9	68.4	46.3	40.8
14	307.3	354.4	84.8	66.1	22.5	22.0
15	38.6	46.6	194.5	151.6	209.4	245.2
17	223.3	268.1	267.9	221.3	34.7	38.1
19	27.0	23.2	49.0	49.0	9.8	9.5
20	277.9	324.0	10.8	13.7	4.0	4.8
21	198.9	244.1	16.8	29.5	0.0	0.0
22	23.5	51.1	0.1	2.9	0.3	0.7
23	1.8	0.6	0.0	0.0	0.0	0.0
24	4.6	4.8	2.2	3.8	0.3	0.0
26	0.0	0.0	5.0	0.2	7.0	7.3
27	8.4	10.4	57.6	35.1	8.1	9.6
28	32.7	39.9	299.4	252.1	38.6	43.0
29	27.4	19.2	236.2	190.3	35.1	30.2
32	0.3	0.0	0.0	0.0	0.0	0.0
34	8.8	6.6	3.6	7.4	0.0	1.0
35	10.4	7.2	1.2	0.0	4.0	2.5
36	2.4	2.1	0.0	0.0	1.5	0.6
37	0.0	0.0	0.0	0.0	0.0	0.0
38	0.0	0.0	0.4	0.0	0.0	0.0
39	0.0	0.0	2.2	2.3	0.0	0.0
40	20.7	14.1	0.2	5.1	16.5	26.1
41	0.0	1.1	39.6	36.3	3.8	3.4
42	0.0	0.0	23.9	22.1	0.0	0.0
43	0.5	0.2	24.0	25.6	0.0	0.2
44	3.3	1.9	9.1	10.1	0.0	0.0
45	1.7	0.0	9.4	19.7	0.0	0.0
46	0.0	2.4	44.7	56.5	0.0	0.0
47	23.9	340.0	334.2	286.1	5.9	11.2
48	0.0	2.2	343.1	294.5	6.0	6.0
49	1.6	3.2	301.5	254.1	32.1	28.3
50	29.6	15.9	401.3	351.3	21.7	47.8
51	9.6	9.2	374.9	325.4	41.7	42.7
52	4.6	2.0	340.9	292.4	29.4	29.9
53	1.7	0.9	8.4	6.0	17.3	14.7

54	0.0	0.0	39.1	37.8	14.5	13.2
55	0.0	0.0	30.5	32.8	12.9	14.6
57	0.0	0.0	5.8	4.6	4.4	2.6
58	0.0	0.0	0.2	0.0	3.9	4.0
59	0.0	0.0	2.9	0.8	0.6	0.1
60	1.0	0.5	0.0	0.0	0.2	0.5
61	4.2	2.7	0.0	0.0	0.0	3.3
62	1.0	0.0	0.0	0.0	1.5	1.6
64	5.7	7.8	41.7	48.6	0.0	0.0
65	0.0	0.0	0.0	0.2	7.3	4.0
66	1.3	0.0	81.3	90.7	9.8	12.4
67	22.4	7.6	7.3	0.0	71.9	58.7
68	0.0	0.6	12.8	6.8	52.1	44.4
69	1.6	2.1	12.4	7.2	103.0	76.0
70	3.8	5.5	25.2	24.6	308.3	345.8
72	10.0	8.6	372.7	323.6	296.0	333.3
73	9.3	8.3	116.5	92.9	303.7	341.1
74	10.3	10.3	19.6	16.9	48.0	49.5
75	0.6	0.7	83.0	67.5	305.6	343.0
77	17.1	13.3	330.0	281.8	273.2	310.1
78	4.3	2.8	363.1	314.2	322.9	360.7
79	297.4	344.3	340.3	291.4	23.1	23.6
82	51.2	38.1	307.0	259.5	239.4	275.6
86	12.1	7.3	27.3	21.7	83.0	69.5
87	26.1	16.5	27.6	9.8	101.2	68.4
89	81.0	58.1	7.0	6.8	41.8	80.2
90	24.3	16.7	4.6	2.5	17.6	14.3
91	5.8	6.0	3.6	6.2	4.7	0.0
92	6.7	6.4	4.2	3.5	2.3	1.0
93	12.8	13.6	0.0	0.0	4.4	2.4
95	5.6	4.9	0.0	4.4	0.0	0.0
96	9.4	8.3	0.0	0.0	4.8	1.7
97	20.9	16.8	0.0	0.0	0.3	1.2
98	21.3	16.6	0.3	0.0	2.4	2.0
99	10.7	8.6	6.3	5.3	2.1	2.3
100	17.4	17.2	0.0	0.1	0.3	2.5
101	68.2	74.8	4.2	1.0	0.4	2.6
102	27.2	29.9	0.0	0.0	0.4	2.2
103	21.3	25.6	0.0	0.0	0.0	0.0

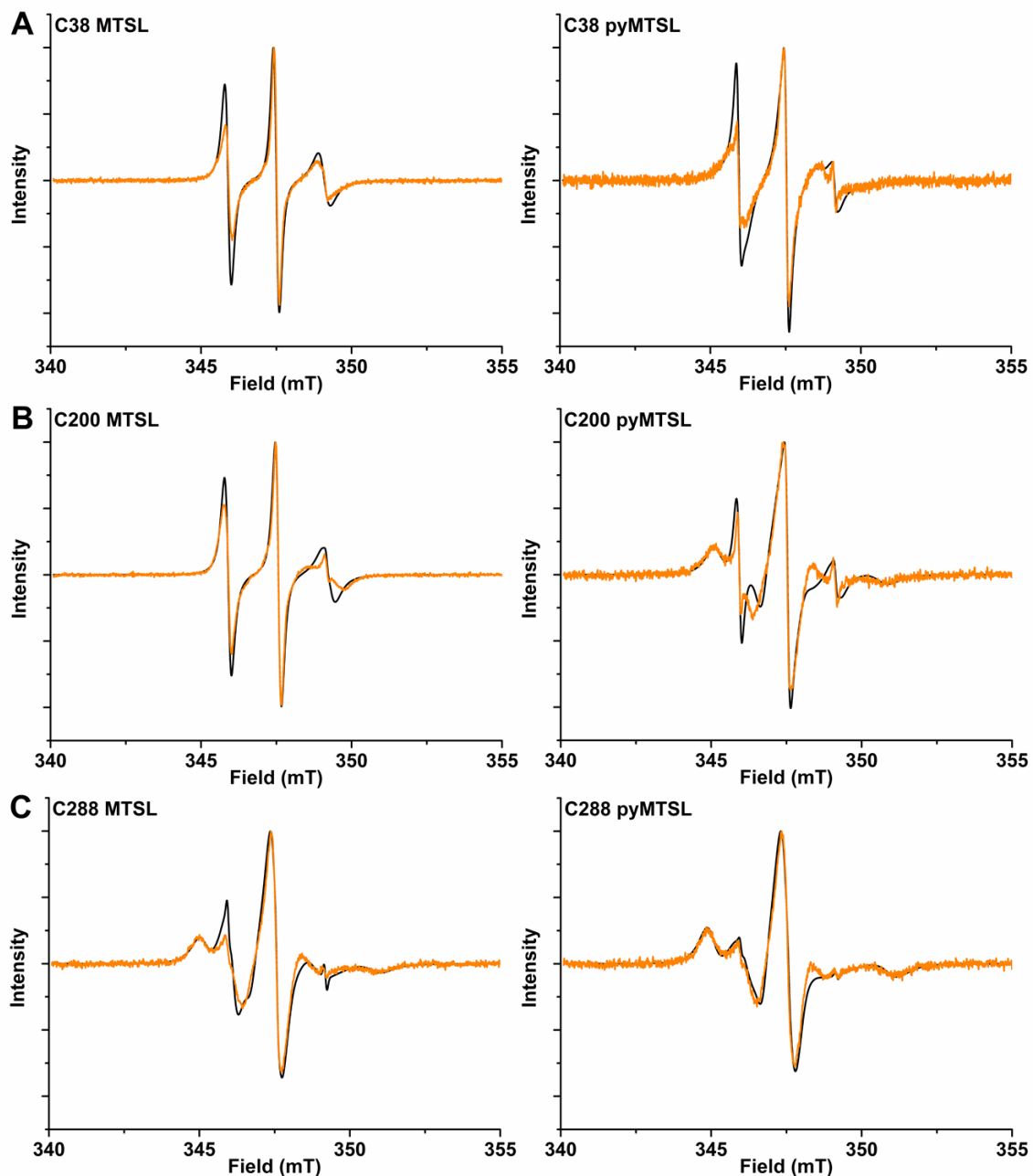


Figure S1: Experimental spectra (orange) and corresponding spectral simulations (black) of MTSL and pyMTSL at positions 38 (A), 200 (B) and 288 (C) on CcP. Simulation parameters, see Table 1 of main text.

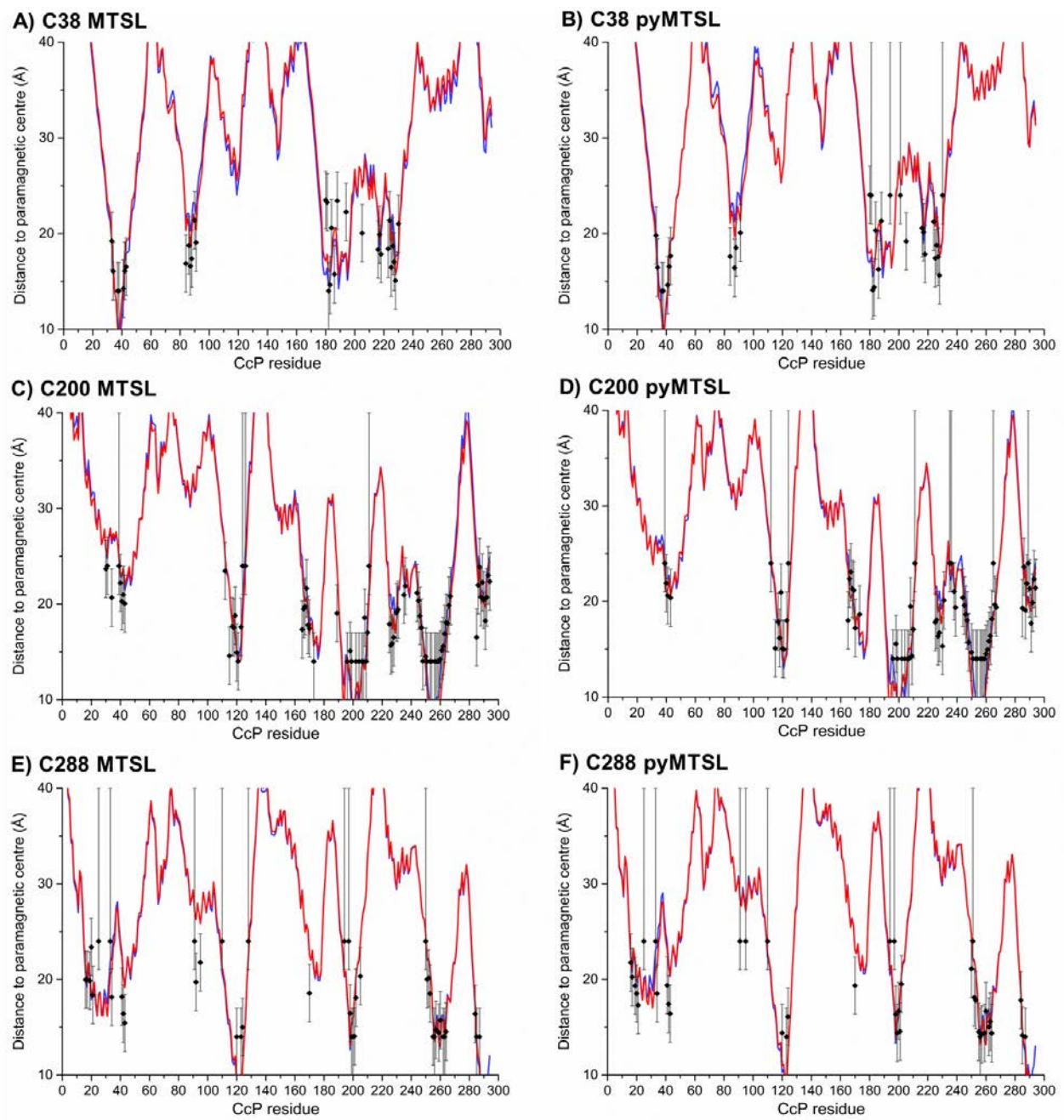


Figure S2: Experimental and back-calculated distances between CcP C128A amide protons and the paramagnetic centre in MTSL or pyMTSL at positions 38 (**A,B**), 200 (**C,D**) or 288 (**E,F**) plotted against the CcP residue number. The black diamonds represent the experimental distances with error bars. Only PREs of residues within 23 Å of the paramagnetic centre were used in the calculations. The average back-calculated distances are also shown as lines for a single SL conformer (red) or an ensemble of four conformers (blue). The PRE were measured while CcP was in a 1:1 complex with Cc.

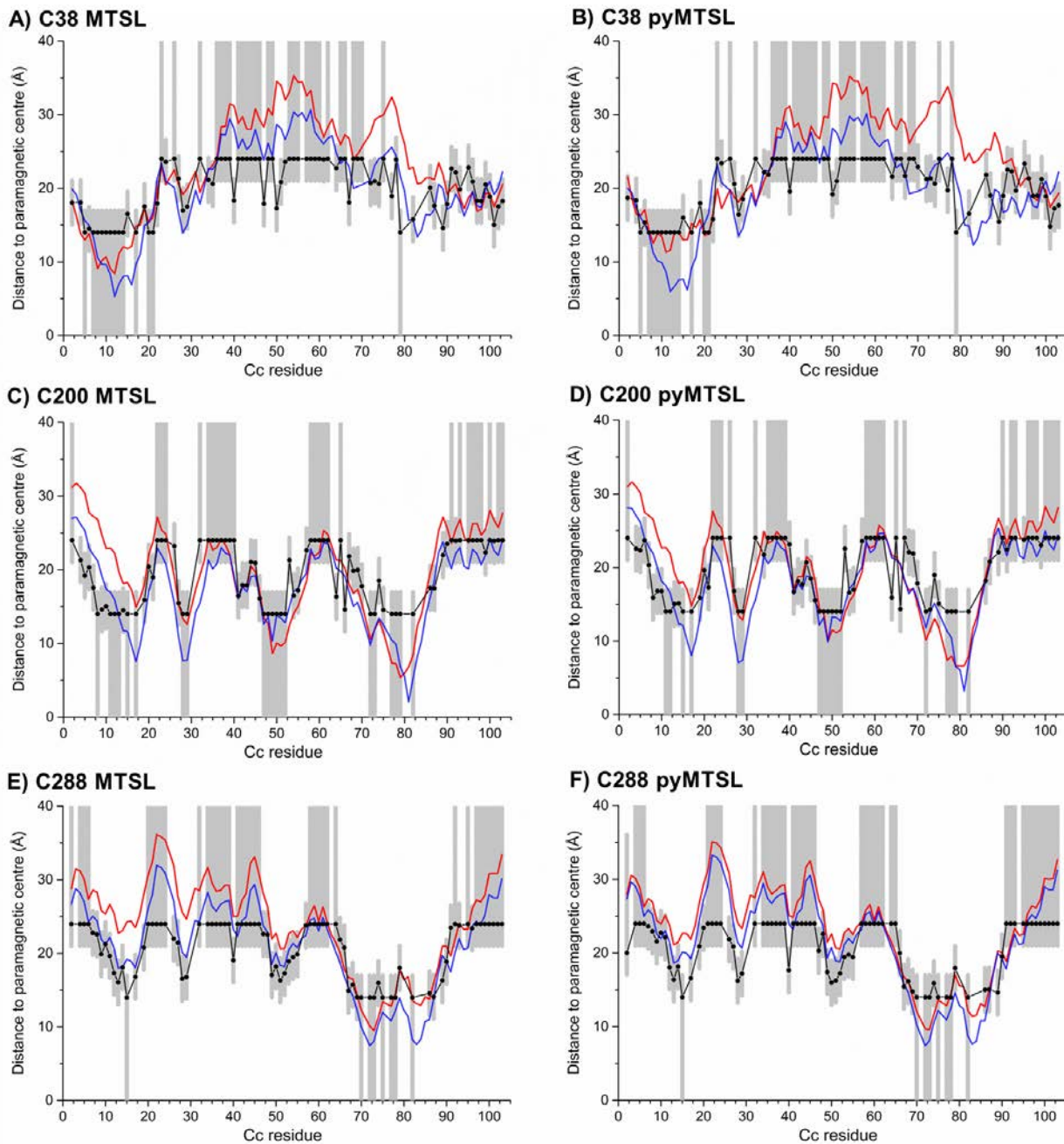


Figure S3: Experimental and back-calculated distances between Cc amide protons and the paramagnetic centre in MTSL or pyMTSL attached at positions 38 (**A,B**), 200 (**C,D**) or 288 (**E,F**) on CcP and plotted against the Cc residue number. The black circles and grey areas represent the experimental distances and error margins, respectively. The average back-calculated distances are shown as lines for a single fixed SL rotamer (red) or a single free SL rotamer (blue). The PRE were measured while CcP was in a 1:1 complex with Cc.

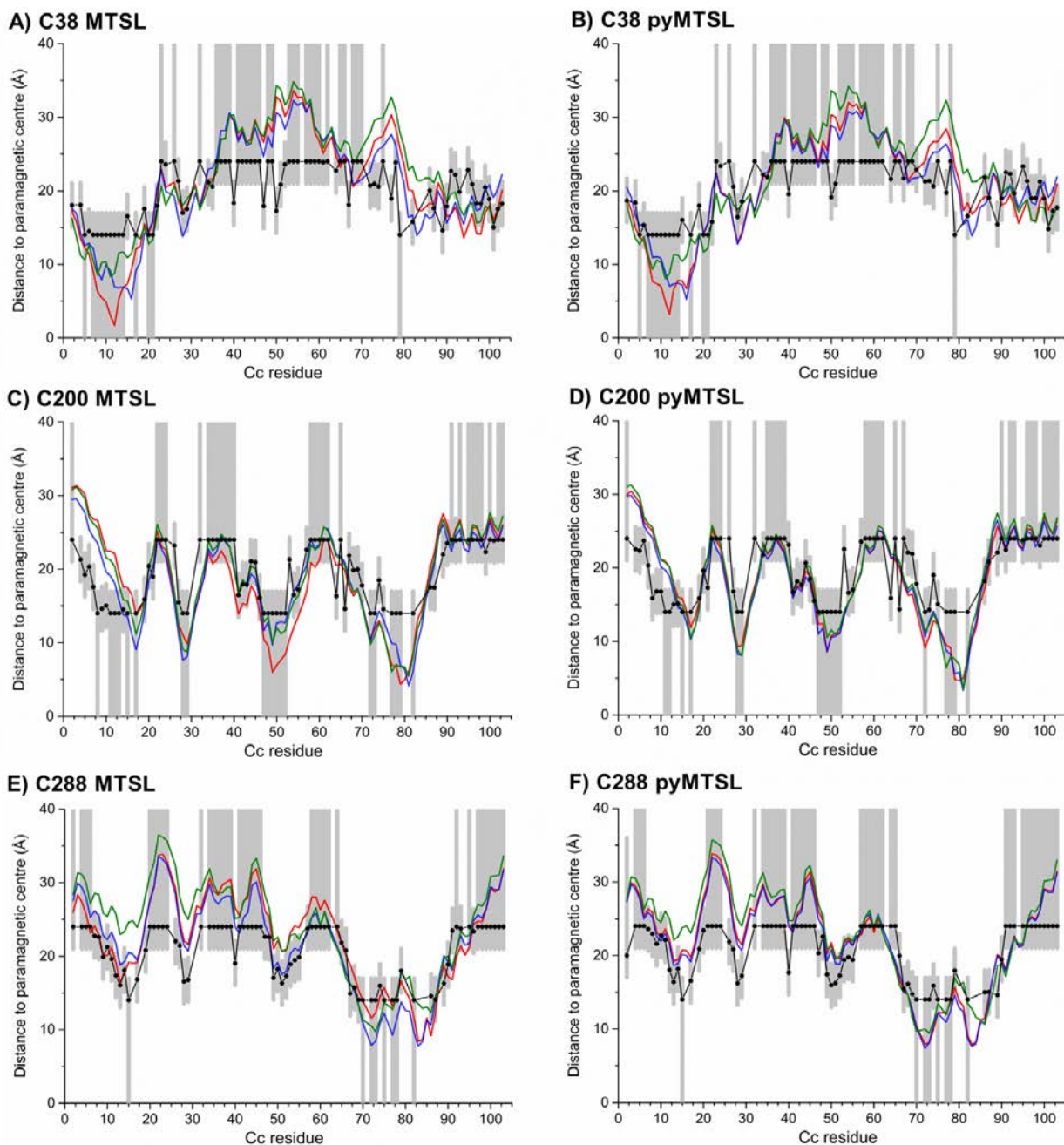


Figure S4: Experimental and back-calculated distances between Cc amide protons and the paramagnetic centre in MTSL or pyMTSL attached at positions 38 (**A,B**), 200 (**C,D**) or 288 (**E,F**) on CcP C128A plotted against the Cc residue number. The black circles and grey areas represent the experimental distances and error margins, respectively. The average back-calculated distances are shown as lines for an ensemble of four SL rotamers that were free to rotate (blue), fixed in random positions (red) or fixed in experimentally determined most favourable orientations (green). The PRE were measured while CcP was in a 1:1 complex with Cc.